Journal of Structural Geology, Vol. 6, No. 6, pp. 727 to 736, 1984
Printed in Great Britain.

0191-8141/84$03.00 + 0.00

A dislocation model applied to slump structures, Ainsa Basin, South Central Pyrenees

S. G. FARRELL

Department of Geology, University College, P.O. Box 78, Cardiff CF1 1XL, U.K.

(*Received* 25 *November* 1983; *accepted in revised form* 16 *April* 1984)

Abstract—Features associated with gravity-induced slumping in deep-water Eocene sediments of the Ainsa basin are described and four aspects are selected as being especially significant. These are: extensional strain, contractional strain, strain overprinting and clastic dykes. Slump strain is interpreted as a consequence of the initiation, translation and termination phases of slump development and is explained in terms of a dislocation model. The initial phase of development involves the propagation of a failure through undisturbed sediment and this imparts a characteristic strain above the décollement surface. Translation of the failed body involves sequential velocity changes which also deform the moving sediment. During the termination phase a type of dislocation, here named an anti-dislocation, migrates along the basal failure when a slump regains cohesion with the substrate. Clastic dykes are interpreted as dewatering structures initiating at basal faults which have associated high pore fluid pressure. Dewatering of slumped décollement sheets may be a significant phase in the termination of movement of failed sediment bodies.

INTRODUCTION

DOWNSLOPE slumping of sediment is now well documented from Recent sequences (e.g. Saxov & Nieuwenhuis 1982) and occurrences in ancient sequences have been reviewed by Allen (1982). Syn-sedimentary disturbances of sediment are relatively common in the stratigraphic record and occur in all depositional environments.

Slope failures (slumping and sliding) due to gravitational instabilities in the sediment pile are a form of pre-lithification deformation that can be classed apart from those deformations caused by tectonic stresses acting on sediment. The identification of large-scale slope failures in ancient deep-water clastic successions that should be present by analogy with Recent sequences (Woodcock 1979a) is a common problem faced by geologists. Factors that mitigate against such identifications are the common tectonic deformation of this type of strata and less than perfect exposure. However, slumps and disturbed zones are often described from ancient deep-water deposits (Pickering 1982, Macdonald & Tanner 1983, Woodcock 1976).

This paper describes some well-displayed examples of gravity induced slumping and attempts to explain the genesis of observed strain states using a dislocation model. The dislocation model describes theoretically the strain associated with the propagation of faults (Elliott 1976, Williams & Chapman 1983). This discussion of soft-sediment deformation will thereby attempt to relate observable strain with the deformation processes that produced the strain. With such an approach individual exposures of soft-sediment deformation may be related on a larger scale to common slope failure events.

GEOLOGICAL SETTING

The deep-water Eocene sediments of the Ainsa basin were deposited in a NNW-trending trough (Nijman & Nio 1975) which was one compartment in a larger basinal system that formed to the south of the developing Pyrenean orogen and was eventually involved in the southward thrusting. Sediment was deposited in the Ainsa basin as turbidites (Mutti 1977), hemi-pelagic marls, slumps and minor olistostromes of the more than 2000 m thick San Vicente formation (van Lunsen 1970).

The San Vicente formation, deformed by south to southwestward thrusting now occurs in part of a trailing imbricate fan (in the sense of Boyer & Elliott 1982) beneath the Cotiella thrust plane. Thrust faults die towards the south and east into asymmetric, S-verging folds with wavelengths of approximately 2 km. Cleavage is rarely developed and minor folds are uncommon. Discrete slumped horizons are folded around these large asymmetric folds and as the slump folds have a wavelength of 2 m or less there is little confusion between tectonic and soft-sediment folds. Structural style within the slumped units will be described from the many good exposures that occur in the area and their locations are shown in Fig. 1.

SLUMP SEQUENCE ORGANIZATION

There are two main slump sequences in the north of the basin which are more than 100 m thick and are traceable for a number of kilometres. They consist of slumped marls (fine-grained turbidites and hemipelagic deposits) and minor slumped sandstone horizons. Slumping in these horizons has disaggregated and partially homogenized the sediments.

Other lithologies present are thin (less than 30 m) olistostromes (with Palaeocene and Cretaceous limestone blocks) and sequences of lenticular sandstone beds (thicker than 1 m) that rarely show slumping. Also there is a thin bedded (less than 20 cm) turbidite lithology that has been informally called the Molinos marls and it is

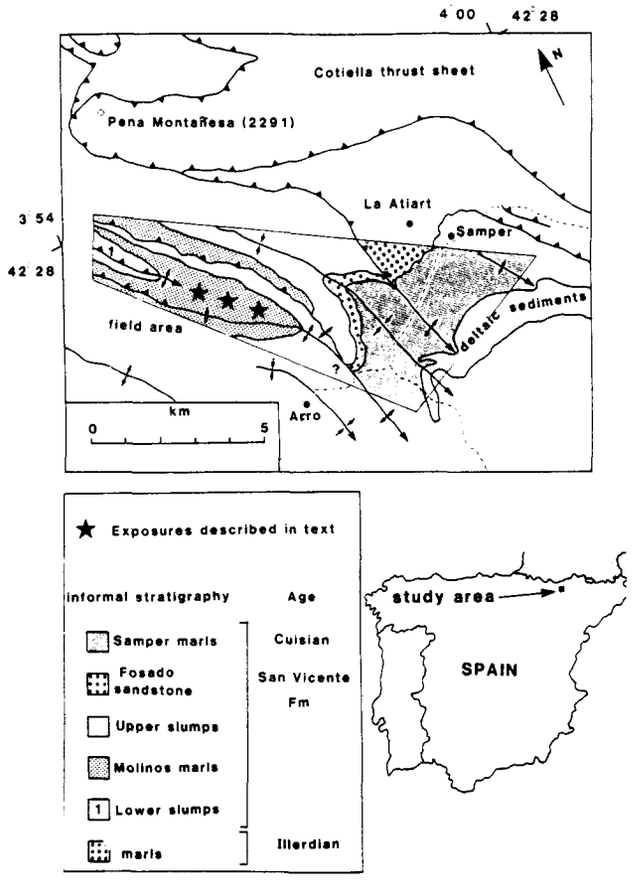

Fig. 1. Schematic geological map of the north east margin of the Ainsa basin, Spanish Pyrenees. Partly after Nijman & Nio (1975), showing localities from which slump measurements were taken.

within this unit that the examples of slumps described in this paper were observed. Slumped horizons comprise about 20% of this unit and where slumps occur in centimetric-scale medium sand/marl couplets (with little grading) then slump structures are particularly well displayed. In contrast, slump structures within thin (cm-scale) graded fine sand or silt/marl beds are often difficult to detect except in water washed surfaces. Slumping that occurred on or near the sea floor is recognized by : (a) ponding of sediment in the irregular topography of the slump sheets (Fig. 2b), (b) erosion of folds and faults before the deposition of overlying beds (Fig. 2c) and (c) rare burrows that cut both slump faults (e.g. Fig. 2a) and folds and indicate that deformation was followed by burrowing. Individual slumps vary in thickness from less than 10 cm to many metres.

The alternation of slumped and undisturbed units implies intermittent instability of the sediment pile in an area of turbidite and hemipelagic sedimentation. Slumping may have been initiated by earthquake activity that accompanied movement on the basin-bounding faults and the propagation of thrust planes to the northeast of the basin.

SLUMP STRUCTURES

Contractional strain

Contractional slump strain is common with slump folds generally occurring above a basal décollement surface (Figs. 2b & c). Commonly, reverse faults that splay from the décollement surface can be seen to cut into the cores of asymmetric folds which developed in response to the basal fault ramping into the sediment pile. Fold vergence is controlled by, and is generally in the same direction as failure propagation. Geometrically, reverse faults are of the piggy-back type (Dahlstrom 1970) with younger thrusts cutting the footwall of the older thrust. Thus, in Fig. 2(b) failure propagation was from the right to left of the diagram. By the process of footwall collapse, movement ceased on the blind reverse faults and the basal failure continued to propagate downslope parallel to bedding. In this case the basal fault failed to cut up to the surface and slip on the fault was accommodated by internal strain in the form of asymmetric folds. In comparison with the thrust geometries of Boyer & Elliott (1982), Fig. 2(b) is an imbricate fan in that most of the ramping faults failed to cut up to an upper roof thrust. It is probable that a roof thrust never existed in this case, the bounding upper surface being the sea floor. The arrangement illustrated in Fig. 2(b) can be shown to have occurred in the surface layers of sediment that were exposed on the sea bed as the synclines became sites of sediment ponding subsequent to the slumping.

Folds above a décollement surface may be symmetrical (Fig. 2c) and information relating to the palaeoslope that can be ascertained from such individual exposures is limited. An erosion surface occurs directly above the slumped unit which planed the upper surface of the slump prior to the deposition of overlying beds.

Extensional strain

Extensional strain takes the form of listric normal faults (Figs. 2a and 3a) and boudinage of competent sandstone layers. Microfaults with a spacing in the order of centimetres and throws of millimetres are common (see Williams *et al.* 1969, Woodcock 1976). These microfaults may be mistaken for a crenulation or pressure solution cleavage. However, thin sections of such microfaults show no truncation or cracking of grains and the fault is only manifested on such a scale by a diffuse (1 mm wide) zone in which there has been a repacking of the sand and silt grains. Normal microfaulting can be seen in units up to 4 m thick. On bedding surfaces the faults produce a strong intersection lineation. The microfaults are generally listric, and root into a basal failure to give extensions that are parallel to bedding. Extensional strain may be partially ductile in character ranging from necking of sandstone layers by small-scale ductile shear zones to bedding which takes on a streaked appearance (in the sense of Jones 1937).

Strain overprinting

Strain overprinting is relatively common in the units investigated. Contractional strain (slump folds and reverse faults) may be overprinted by extensional strain

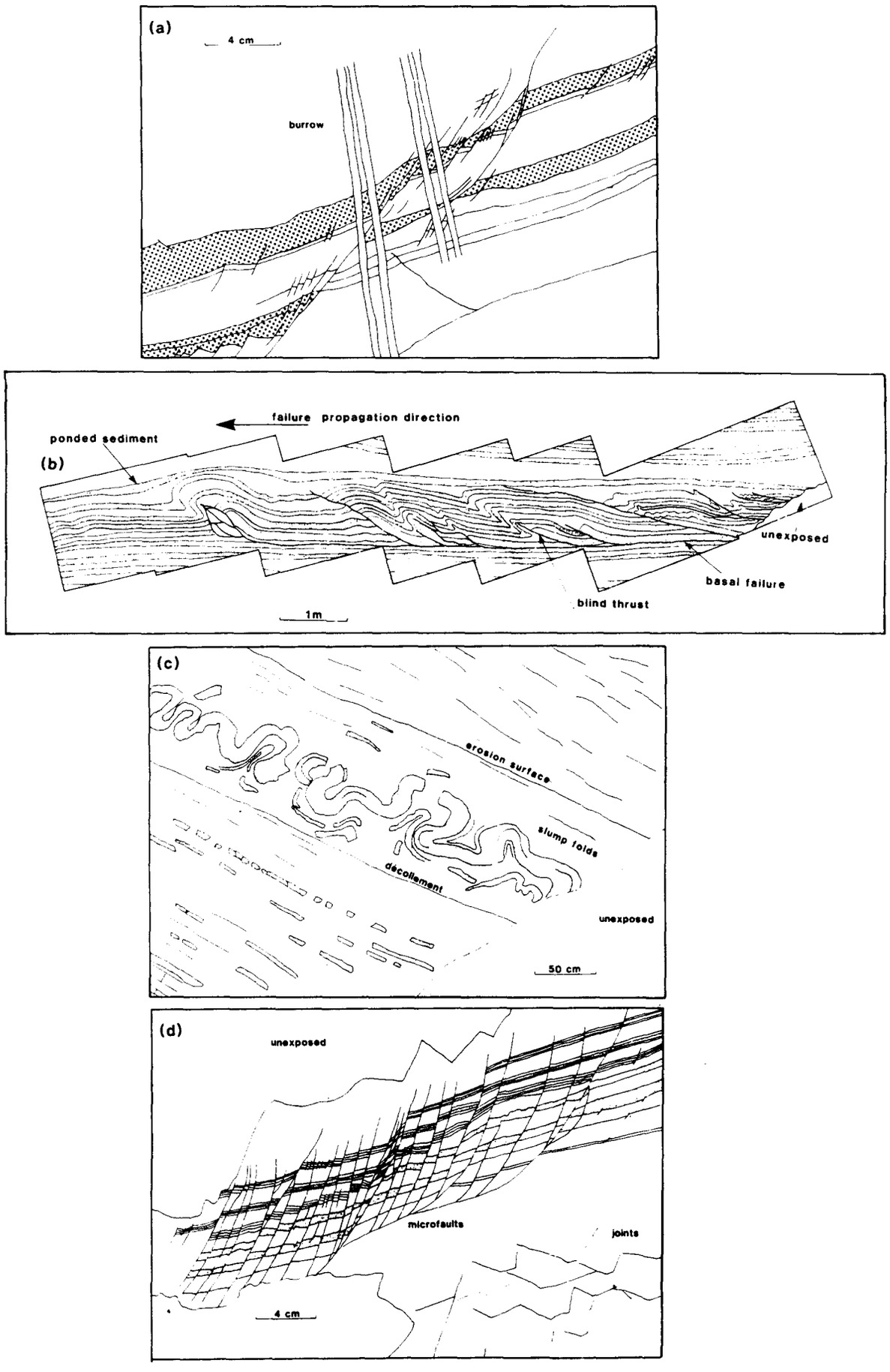

Fig. 2(a) Normal faults, some listric, cut by burrows. (b) Slump unit with contractional strain. Vergence direction of the folds indicates that they propagated from right to left. (c) Nearly symmetrical slump folds in a sandstone bed. These folds show signs of disaggregation. Beneath the slump is a basal décollement surface and above it a planar erosion surface upon which sediment was deposited. (d) Pervasive normal microfaults.

(normal faults and boudinage) (Fig. 3a). Overprinting of extensional faults by contractional features is less common. Figure 3(b) displays the juxtaposition of contractional (folds and reverse faults) and extensional strain (boudinage and normal faults). Superimposed faults may be mistaken for axial-plane cleavages as the strike of microfault planes is often similar to that of slump fold axial planes. Strain overprinting has been reported by workers in other areas (Jones 1937, Williams & Prentice 1957, Woodcock 1976). Sets of conjugate normal slump faults with variably intersecting strikes are common in the Ainsa basin both associated with and separate from slump folds. These features have also been described by Thompson (1973) and Biju-Dival *et al.* (1974) in other areas.

A palaeoslope inferred from slump strain

The orientation of slump structures shows a systematic arrangement which is repeated in successive slump sheets. This is illustrated by stereoplots of selected structural elements from these slump sheets (Figs. 4a–c). Poles to faults (both normal and reverse) and plunges of slump fold axes have been plotted. The movement direction of the slump sheet is assumed to have been perpendicular to the mean axis of slump folds (Jones 1940, Woodcock 1979b). It is assumed that not all fold vergence and facing directions will give the downslope direction as folds with opposing vergences are often encountered (e.g. Fig. 3b). The plunge of slope fold axes is generally low and shows a distribution around a NW to SE azimuth. The mean fold axis is 8–150° (±5°) which is used as an estimate of palaeoslope strike. Although a significant number of folds verge towards the NE the majority of asymmetric folds verge towards the SW which is the inferred palaeoslope. This result is supported by the palaeogeographic reconstruction of the basin (Nijman & Nio 1975). A mean value of slump reverse fault strikes is 151° (±5°) with most faults dipping towards the NE, again indicating a palaeoslope towards the SW. Normal faults show a greater spread of values than the reverse faults as the conjugate set is often developed. The mean fault value gives a palaeoslope strike at 135° (±5°). If it is assumed that the majority of faults dip downslope then this indicates a palaeoslope towards the SW.

Clastic dykes

Another characteristic feature of the Ainsa basin slumps is the presence of clastic dykes that lie along or diverge from slump failure planes. The material filling these dykes is brecciated sediment derived from the dyke walls and the matrix is either mudstone or finely comminuted sediment clasts. Conspicuously absent are breccia clasts set in a calcite or quartz cement that are often found in tectonically formed breccias. These dykes commonly show preferred orientations which approximately follow the trend of nearby normal faults. Such orientations are probably due to the dykes forming along extensional fractures. This is evident in Fig. 3(c) where breccia dykes are associated with a slump décollement surface (indicated as a fault gouge). This failure plane was probably a horizon of high fluid pressure from which fluid escaped along conjugate normal faults, brecciating the walls of the fractures. In other parts of the area clastic dykes and other dewatering structures can be seen emanating from reverse slump faults and cutting across slump folds. Such clastic dykes, on reaching the sea floor would give rise to sand volcanoes and clast-filled fissures.

DISCUSSION

A dislocation model

A somigliana dislocation model has been used to describe the propagation of faults in general (Eshelby 1973) and reverse faults in particular (Elliott 1976, Hossack 1983, Williams & Chapman 1983). Such a model assumes that during faulting a fault tip line (Boyer & Elliott 1982) spreads out radially from a point of initial failure (Fig. 5a). Material enclosed within the tip line has slipped and is faulted, outside the tip line the material is unslipped. Slip on the fault is at a maximum at the initial failure point (Williams & Chapman 1983) and nil at the tip line (Fig. 5b). There is a zone of ductile accommodation between the slipped and unslipped material associated with the fault tip and this is termed the ductile bead (Elliott 1976). The ductile bead associated with contractional strain is often expressed as folding (Elliott 1976, Williams & Chapman 1983). Slip on the fault must be taken up as strain within the faulted material and a characteristic strain is imparted at the fault tip as it propagates through the material. The magnitude of this strain will depend on the fault length to slip ratio (Williams & Chapman 1983) (Fig. 5c). The geometry of the ductile bead will depend on the fault propagation direction in relation to the slip direction. In a section through the initial failure, parallel with the slip direction, there will be extensional strain where the dislocation propagates in the opposite direction to the slip direction. Contractional strain will occur where the dislocation propagates in the same direction as the slip direction (Figs. 6a & b). In slope failures the slip direction will generally be downslope. The zone in which the dislocation propagates in the opposite direction to the slip (extensional strain) will be upslope of the initial failure point. Contractional strain will develop downslope of the initial failure. Quantitatively, there will be a volume of contractional strain and a volume of extensionally strained material. The line between these zones was originally at right angles to the slip direction and passed through the initial point of failure (Figs. 6a & b). Material lines that were initially parallel to the slip direction remain so, while those at other angles to the slip direction are rotated towards the slip direction by some characteristic angle dependent on the fault length/slip ratio.

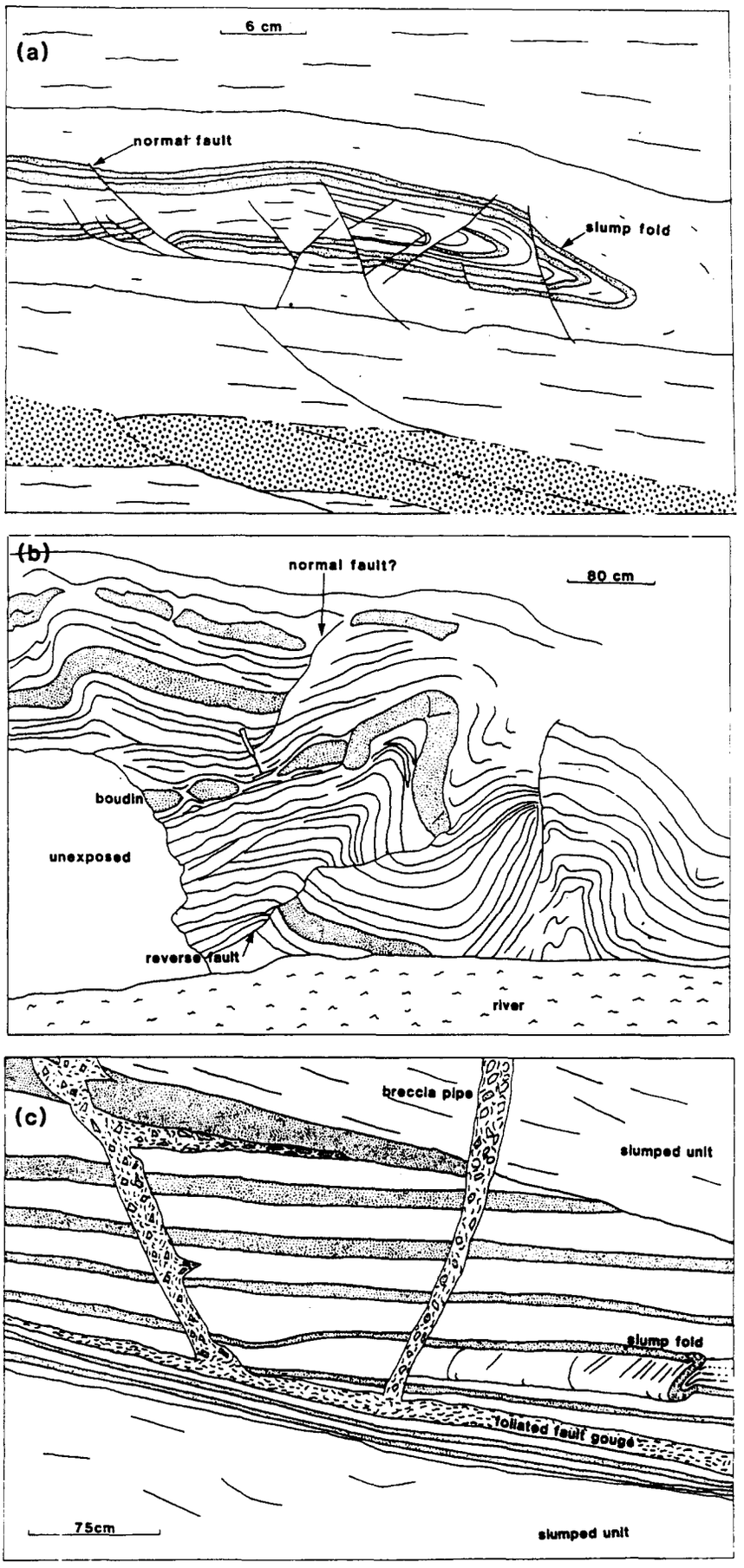

Fig. 3(a) Contractional slump fold cut by later extensional faults. (b) Contractional slump strain (reverse faults and asymmetric folds) associated with extensional strain (normal faults and boudins). (c) Clastic dykes that root into a slide failure plane. Dykes are parallel to nearby normal faults.

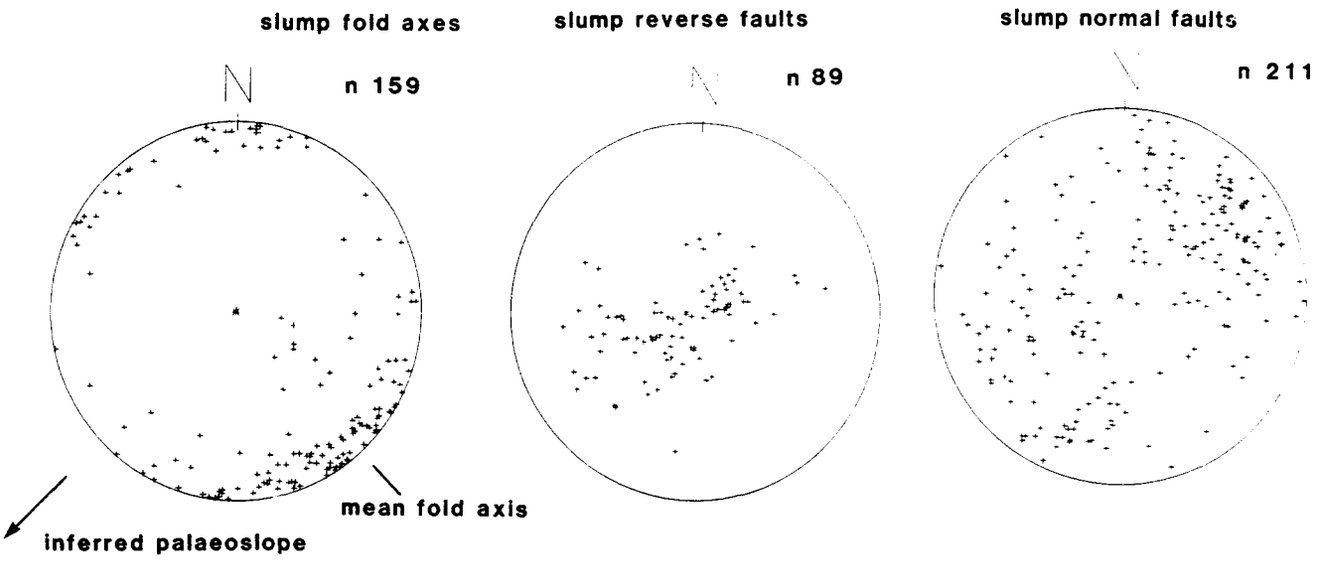

Fig. 4. Equal-area stereoplots of slump data.

A dislocation model applied to slumps

Seismic sections of submarine slumps (e.g. Lewis 1971) are characterized by a basal failure above which the material is strained. Strain is predominantly contractional at the downslope end and extensional at the upslope end (Fig. 6c). This is similar to the theoretical cross-section of a dislocation loop already outlined (Fig. 6a). Thus in slumps extensional and contractional strain can be related to an upslope or downslope position in relation to the initial failure point. In such a model, Figs. 2(b) & (c) and 3(b) represent the contractional region of the slump unit downslope of the initial failure. Figure 2(b) illustrates the tip line which is the point between faulted and unfaulted sediment shown at the left of the diagram. Each asymmetric fold with a fault dying into it is an expression of the ductile bead in front of a developing fault. In this case footwall ramp collapse arrested further development of the faults. Figure 2(c) shows contraction above a décollement surface with little obvious vergence of folds. This is consistent with being in the contractional part of a slumped unit. Figures 3(a) & (b) show mainly contractional strain features formed downslope of an initial failure but there has been a phase of extensional strain superimposed on the slump at some later stage in its development.

Figures 2(a) & (d) can be assigned to an extensional strain zone upslope of the initial failure point. Some slumps appear to have a characteristic strain (fault spacing, fold wavelength) throughout a particular sheet and this is also consistent with a dislocation model which predicts constant strain above the décollement surface for constant slip/fault length ratios. If a conjugate set of contractional faults should develop in a slump sheet,

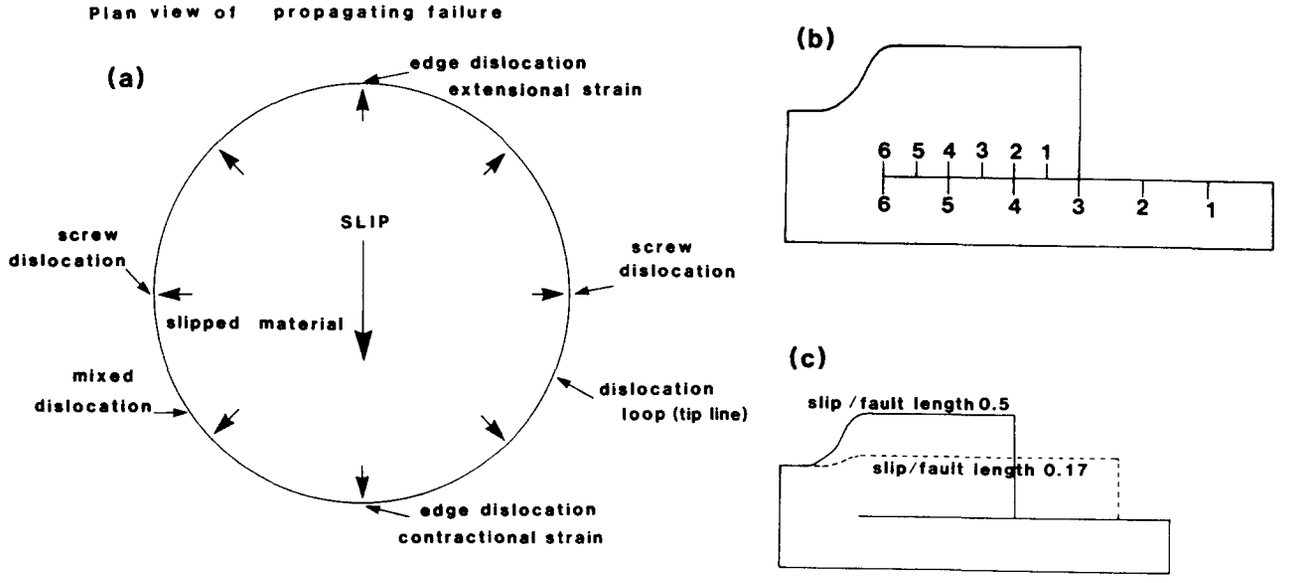

Fig. 5(a) Plan view of theoretical propagating failure. (b) Theoretical fault with markers that show slip to have been at a maximum at the rear of the unit and zero at the fault tip. (c) Variations in slip/fault length. A high slip/fault length ratio produces high strain, low slip/fault length ratios produce low strain.

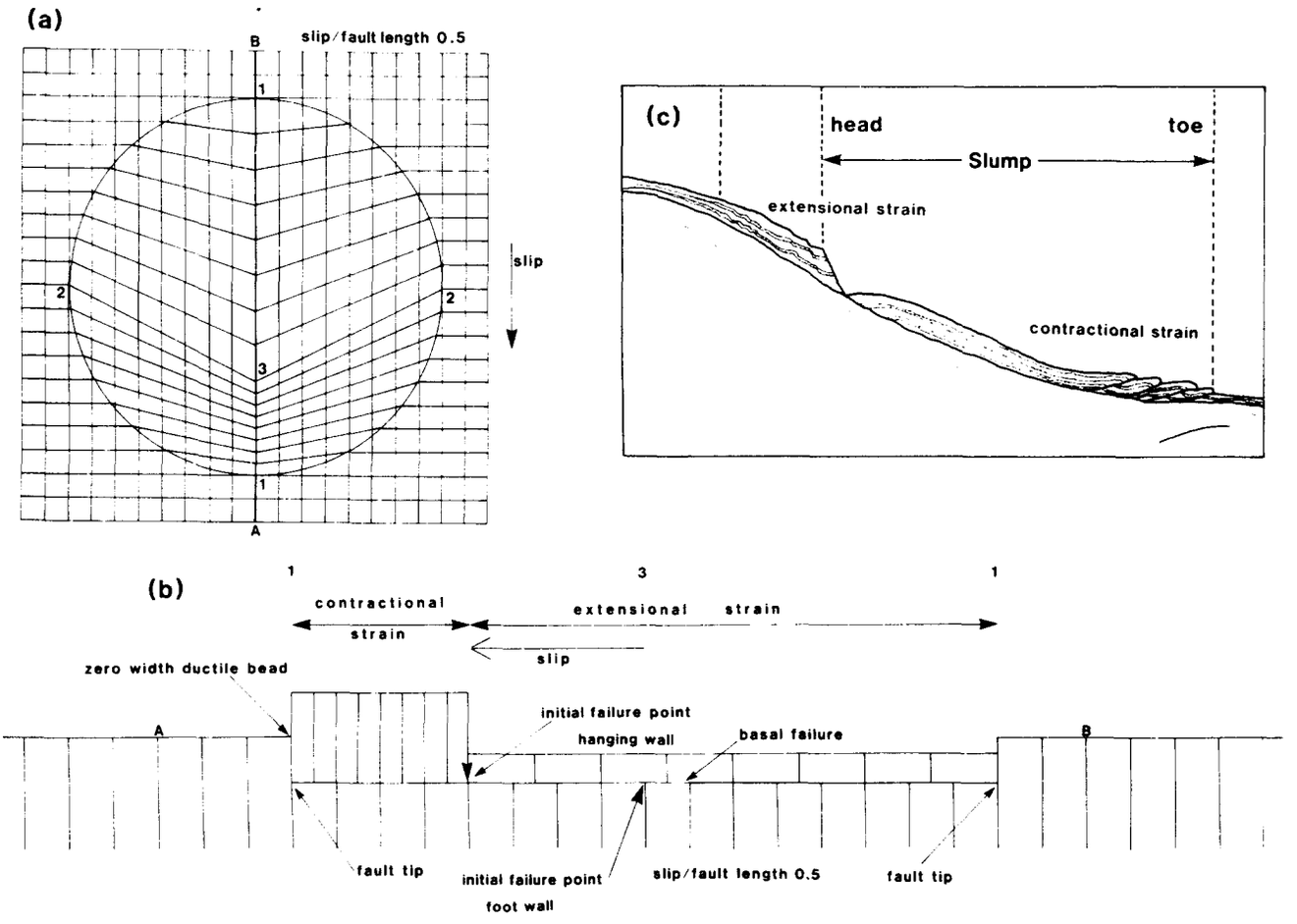

Fig. 6(a) Plan view of a failure plane and the effect of the propagating failure on material lines. 1, edge dislocations; 2, screw dislocations; 3, initial failure point and change from contractional to extensional strain. (b) Cross section through the failure loop of Fig. 6(a) from A to B. Area has been maintained from that originally present. In the slip direction the fault propagates with a contractional strain wave. Numbered features as in (a). (c) Idealised cross section of a submarine failure as interpreted from seismic sections (after Lewis 1971, fig. 2).

then folds associated with upslope propagating faults will verge upslope. Those faults which propagate in the opposite direction to the bulk transport direction are analogous to back thrusts in orogenic belts. Folds which have opposing sense of vergences can be seen in Fig. 3(b). In examples of subaerial failures (Lajoie 1972, Stone 1976) contractional strain features in plan view are seen to be convex downslope. Minor extensional features are concave downslope. This may be due to a combination of the rotation of material lines (e.g. fold axes) into parallelism with the slip direction and the fact that strain features will tend to form normal to a radially propagating dislocation. A dislocation model also predicts that the outcrops of contractional features are concave downslope and extensional features concave upslope. Fold hinge lines and fault strikes from the slump sheets in the Ainsa basin, plotted in Figs 4(a–c), are consistent with such concave/convex distributions about mean values. A simple dislocation model will explain the strain that is produced during the propagation of a failure and this type of strain is seen preserved in simple failed bodies in seismic sections (Fig. 6c). However, much slump strain is demonstrably complex (such as strain overprinting) and probably occurs during the translation of the failed unit. In the following section a model of slope failure is proposed using the application of dislocation theory in zones of high pore fluid pressure.

Strain history of slump sheets

A flow diagram (Fig. 7) shows the possible developmental pathways of a failed sediment mass. If during a slip event the gross cohesion of the body with the substrate is not lost then this is described as a creep event. In a creep event the area undergoing active slip is always less than the total area of the décollement surface. Features such as those illustrated in Fig. 7 can be explained by the initiation phase of slumping and one creep event may have given rise to all the observed strain. If the unit loses gross cohesion with the substrate, it will enter the translation part of the flow diagram. During the translation phase further strain states may be superimposed on those developed during initiation.

Slump strain overprinting during translation of the failed sediment mass

While the sediment body is moving downslope, sequential velocity changes will tend to cause strain waves to propagate through the body and superimpose

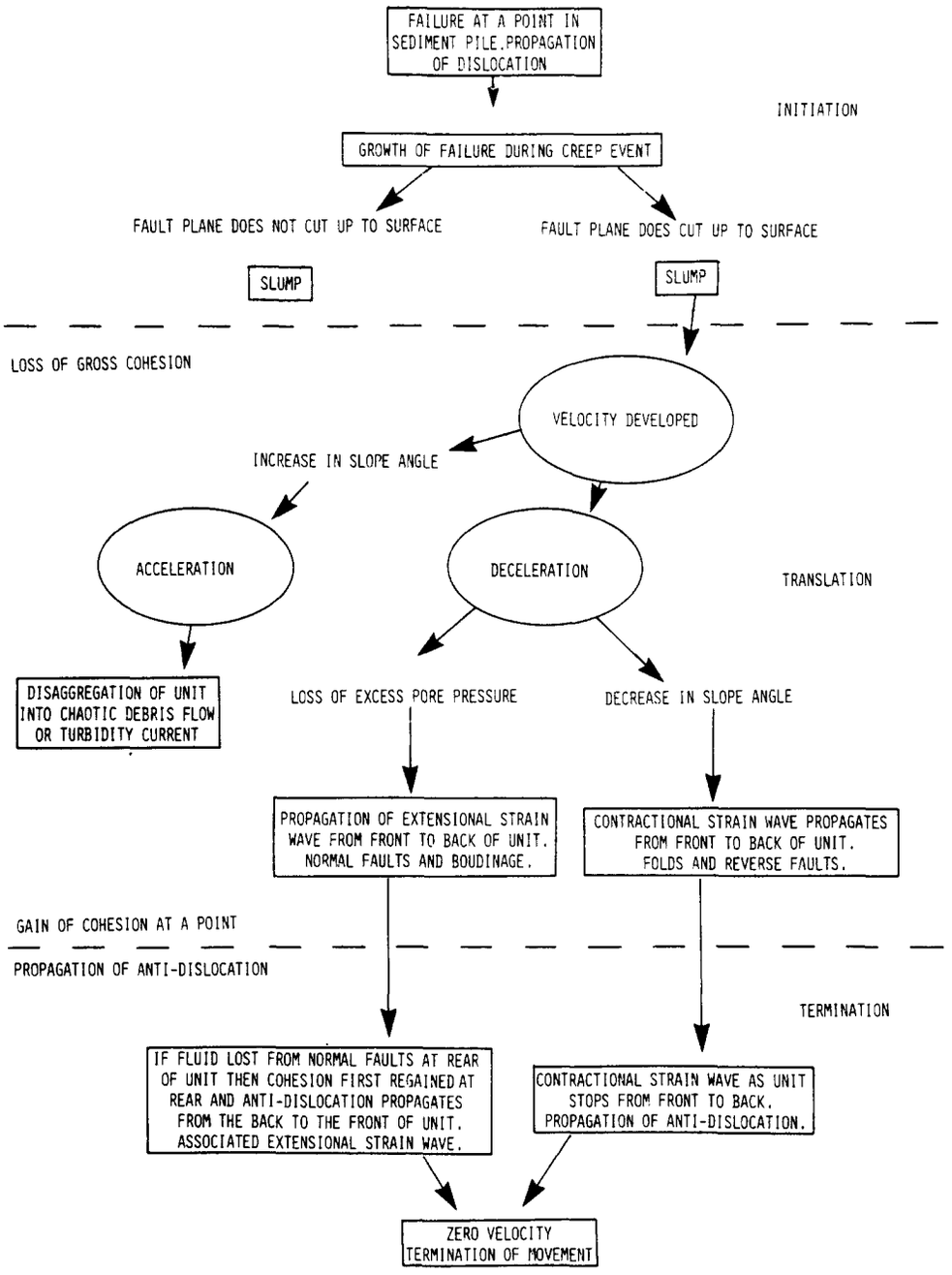

Fig. 7. Flow diagram outlining some evolutionary possibilities of a downslope failure.

strain on that already present in the sediment mass. If the velocity reaches a critical level disaggregation will take place and the movement will continue as some type of debris flow. Debris flows are common in the Ainsa basin, often with disaggregated sandstone beds showing slump strain (extensional and contractional) in a marl matrix. If the velocity drops, cohesion with the substrate may be regained and so the slump will enter the termination phase shown in Fig. 7.

Strain overprinting due to termination of movement: anti-dislocations

In order for a failed sediment mass to come to rest the shear strength of the basal décollement surface must once again exceed the shear stress on it. This may result from either an increase in shear strength or a decrease in shear stress.

A decrease in shear stress can be expected when there is a change to a lower slope which allows the shear stress to drop below a critical level such that the body comes to rest. This stopped region will begin at the front of the slump and propagate to the back (Fig. 8a). On the basal décollement surface there will be slipping and nonslipping regions and the contact between these two regions will again be a type of dislocation. In the case of the slipping material regaining cohesion with the substrate and the area of the fault undergoing active slip decreasing, it is proposed that the line between slipping and unslipping material should be referred to as an anti-dislocation. Like a dislocation, the nature of deformation produced by the propagation of the anti-dislocation

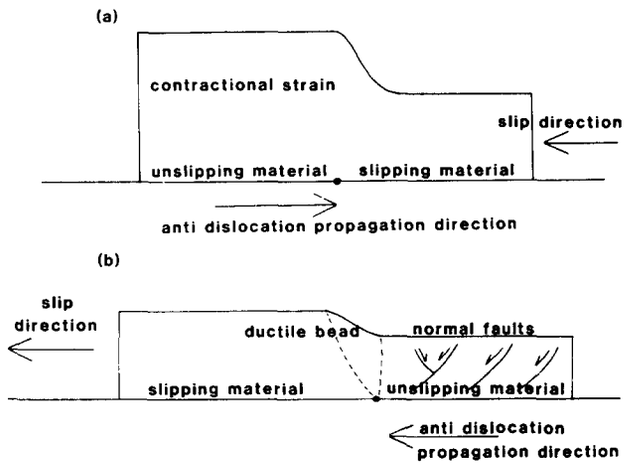

Fig. 8(a) Anti-dislocation propagation with associated contractional strain wave during final phase of slump development. (b) Anti-dislocation propagation with associated extensional strain wave during final phase of slump development.

depends on the direction of its propagation in relation to the bulk transport direction.

In the case of a unit stopping at the base of a slope, slip continues upslope of the anti-dislocation. The anti-dislocation migrates up the failure surface until the whole unit has stopped (Fig. 8a). Associated with the anti-dislocation will be a ductile bead and a contractional strain wave.

If initial failure occurs in a region of elevated pore pressure then major fractures produced by the failure will provide conduits for fluid to escape and will allow a drop in pore pressure and hence a gradual increase in shear strength on the basal décollement surface.

Fluid can escape from the front, sides and rear of the failure but as the initial failure event has left the rear portion of the slump cut by normal faults, fluid may escape preferentially from the rear of the unit through these fractures. This increases the shear strength of the sediment at the rear of the unit causing the upslope end to stop. As the front of the unit is still moving, an anti-dislocation will propagate from the rear to the front of the failed mass. In this case it will have an extensional strain wave associated with it (Fig. 8b). This appears to have commonly occurred within the slumps studied. Extensional strain overprinting contractional is more common than vice versa (Figs. 3a & b). As the sheet extends with the downslope propagation of the extensional strain wave additional fractures can develop along which fluid may escape and this may lead to the migration of a locus of dewatering from the back to the front of the sheet.

Localized rapid loss of pore pressure can give rise to clastic dykes (e.g. Fig. 3c) and injection structures and on the surface of a failed unit may be manifested as sand volcanoes. A migrating point of dewatering has been interpreted by Gill & Kuenen (1958) and Gill (1979) and may well be produced by such a mechanism. Gill & Kuenen (1958) also noted the common association of sand volcano vents with slump faults. Thus, although failed sediment bodies will commonly come to rest at the base of a slope they may also come to rest on the slope itself by the loss of their excess pore pressure.

CONCLUSIONS

There are certain morphological associations in semicoherent downslope mass movements that indicate a common genesis. These features are: (1) rapid changes spatially from contractional to extensional strain, (2) the overprinting of strain states, (3) pervasive microfaulting, (4) clastic dykes and injection structures and (5) sand volcanoes. A dislocation model which can be applied to any fault generating process can be applied to the development of the basal décollement surface in slope failures. This model successfully accounts for the initial distribution of strain in simple failure events. Strain overprinting can be explained by the propagation of dislocations during translation of the body and a special dislocation, an anti-dislocation, will propagate and redeform the sediment as it regains cohesion with the substrate.

Slumps are often considered to have come to rest at the base of a slope but consideration of the final strain overprint which is often demonstrably extensional may indicate that the unit came to rest on the slope by dewatering at the rear of the unit. Extensional strain above a décollement surface is as frequent a feature of and evidence for downslope movement as are the more commonly described contractional strain features. For a circular dislocation loop the area of extensionally strained sediment will be much greater than the area of the contractional portion (Fig. 6b). However, dislocation loops need not be circular or symmetrical about the initial failure. If downslope fault propagation is significantly greater than slope-parallel propagation, material lines are further rotated towards the slip direction. Different slip/fault-length ratios in the extensional and contractional strain zones will give rise to different strains above the décollement surface and the extensional zone may be small due to the basal failure rapidly cutting up to the surface.

Downslope failures can occur on all scales from a few millimetres to several kilometres of failed sediment. The larger failures in their contractional part may be difficult to distinguish by style of deformation alone from tectonic contractional strain. Using this model it may be possible to map out failed units with more confidence and by using a predictive strain theory distinguish the slump strain from that that will be expected from tectonic deformation.

Acknowledgements—I would like to acknowledge Phil Allen, Mike Brooks and Mick Fischer for criticising early drafts of the manuscript and Graham Williams for many of his ideas which have been used in this paper. I would like to thank Djin Nio without whom this research would not have been feasible and Paula Westall for typing. This research was carried out with a Shell Oil Company Scholarship.

REFERENCES

Allen, J. R. L. 1982. *Sedimentary Structures. Their Character and Physical Basis. Volume 2*. Elsevier, Amsterdam.

Biju-Duval, B., Deynoux, M., & Rognon, P. 1974. Essai d'interpretation des "fractures en gradins" observees dans les formations glacieres pre-Cambriennes et Ordoviciennes du Sahara. *Revue Géogr. phys. Géol. dyn. Paris* **16**, 503–512.

Boyer, S. E. and Elliott, D. 1982. Thrust systems. *Bull. Am. Ass. Petrol. Geol.* **66**, 1196–1230.

Dahlstrom, C. D. A. 1970. Structural geology in the eastern margin of the Canadian Rocky Mountains. *Bull. Can. Petrol. Geol.* **18**, 332–406.

Elliott, D. 1976. Energy balance and deformation mechanisms of thrust sheets. *Phil. Trans. R. Soc.* **A283**, 289–36.

Eshelby, J. D. 1973. Dislocation theory for geophysical applications. *Phil. Trans. R. Soc.* **A274**, 331–338.

Gill, W. D. & Kuenen, P. H. 1958. Sand volcanoes on slumps in the Carboniferous of County Claire, Ireland. *Q. Jl. geol. Soc. Lond.* **93**, 441–460.

Gill, W. D. 1979. Syndepositional sliding and slumping in the West Clare Namurian Basin. Ireland. *Spec. Publs geol. Surv. Ir.* **4**, 1–31.

Hossack, J. R. 1983. A cross section through the Scandinavian Caledonides constructed with the aid of branch line maps. *J. Struct. Geol.* **5**, 103–111.

Jones, O. T. 1937. On the sliding and slumping of submarine sediments in Denbighshire, North Wales during the Ludlow Period. *Q. Jl geol. Soc. Lond.* **93**, 241–282.

Jones, O. T. 1940. The geology of the Colwyn Bay district: a study of submarine slumping in the Salopian Period. *Q. Jl geol. Soc. Lond.* **95**, 335–382.

Lajoie, J. 1972. Slump fold axis orientations. An indication of palaeoslope? *J. sedim. Petrol.* **42**, 584–586.

Lewis, K. B. 1971. Slumping on a continental slope inclined at 1–4 degrees. *Sedimentology* **16**, 97–110.

van Lunsen, H. A. 1970. Geology of the Ara-Cinca Region, Spanish Pyrenees, Province of Huesca. *Geol. Ultraiectana* **16**, 1–119.

Macdonald, D. I. M. & Tanner, P. W. G. 1983. Sediment dispersal patterns in part of a deformed Mesozoic back arc basin of south Georgia, South Atlantic. *J. sedim. Petrol.* **53**, 83–104.

Mutti, E. 1977. Distinctive thin bedded turbidite facies and related depositional environments in the Eocene Hecho Group (South-Central Pyrenees, Spain). *Sedimentology* **24**, 107–131.

Nijman, W. & Nio, S. D. 1975. The Eocene Montaña delta in the sedimentary evolution of the Paleogene South Pyrenean Basin. In: *Sedimentary Evolution of the Paleogene South Pyrenean Basin* (edited by Rosell, J. & Puigdefabregas, C.). *9th Int. Congr. Sedim., Nice*, Field trip 19, 1–19.

Pickering, K. T. 1982. A Precambrian Upper Basin-Slope and Prodelta in Northeast Finnmark, North Norway—a possible ancient upper continental slope. *J. sedim. Petrol.* **52**, 171–186.

Saxov, S. & Nieuwenhuis, J. K. (Eds) 1982. *Marine Slumps and other Mass Movements*. Plenum Press, New York.

Stone, B. D. 1976. Analysis of slump slip lines and deformation fabric in slumped Pleistocene lake beds. *J. sedim. Petrol.* **46**, 313–325.

Thompson, A. 1973. Soft sediment faults in the Tensus Formation and their relationships to paleoslope. *J. sedim. Petrol.* **43**, 525–528.

Williams, B. J. & Prentice, J. E. 1957. Slump structures in the Ludlovian rocks of North Herefordshire. *Proc. Geol. Ass.* **68**, 286–293.

Williams, G. D. & Chapman, P. 1983. Strains developed in the hangingwalls of thrusts due to their slip/propagation rate: a dislocation model. *J. Struct. Geol.* **5**, 563–572.

Williams, P. F., Collins, A. R., & Wiltshire, R. G. 1969. Cleavage and penecontemporaneous deformation structures in sedimentary rocks. *J. Geol.* **77**, 415–425.

Woodcock, N. H. 1976. Structural style in slump sheets. Ludlow series, Powys, Wales. *J. geol. Soc. Lond.* **132**, 399–415.

Woodcock, N. H. 1979a. Sizes of submarine slides and their significance. *J. Struct. Geol.* **1**, 137–142.

Woodcock, N. H. 1979b. The use of slump structures as palaeoslope orientation estimators. *Sedimentology* **26**, 83–99.